ISBN: 978-3-95450-247-9 ISSN: 2673-5490 doi: 10.18429/JACoW-IPAC2024-TUPR47

# MAGNETIC DESIGN OF NON-LINEAR KICKER FOR ESRF-EBS

C. Benabderrahmane†, D. Baboulin, T. Brochard, M. Dubrulle, G. Le Bec,
M. Morati, J-L. Pons, S. White, ESRF, Grenoble, France

## *Abstract*

The ESRF-EBS injection is performed with a standard off-axis injection scheme consisting of two in-air septa S1/2, one in vacuum septum S3 and four kicker magnets K1 to K4 to generate the injection bump. We can achieve 80% efficiency with this scheme. Despite many modifications and adjustments which allow the reduction of the perturbation, some beamlines are still affected. The Non-Linear Kicker (NLK) could be a solution to this problem because it acts only on the injected beam. This paper reports on the magnetic design of the NLK, including the octupole like Magnetic field simulations, mechanical tolerance optimisations and the presentation of a prototype magnet to validate the magnetic design and mechanical assembly.

## INTRODUCTION

The European Synchrotron Radiation Facility (ESRF) is an intense X-ray source located in Grenoble, France. It is a centre of excellence for fundamental and innovation-driven research. ESRF owes its success to the international cooperation of 22 partners, of which 13 are members and 9 are scientific associations.

A major upgrade project known as ESRF-EBS was launched in 2015 and achieved in 2020. It aims to reduce the horizontal emittance from 4 nm.rad down to less than 140 pm.rad. The brilliance of ESRF-EBS is increased by a factor of 30 compared to the former one, mainly due to this drastic decrease of the horizontal emittance. The present Hybrid Multi Bend Achromat lattice replaced the Double Bend Achromat one [1].

After a few months of commissioning, the ESRF-EBS machine is in User Service Mode (USM) operation since mid-2020. It is using the standard four kickers of the old machine, which allows the achievement of 80% injection efficiency in USM [2]. Unfortunately, the normalized residual injection perturbations are approximately an order of magnitude larger than for the previous machine, mainly due to the reduction of the beam size. Despite many modifications which allowed the reduction of a big part of these perturbations, the feedback from beamline experiments mentioned that a factor of 2 of perturbation reduction is still necessary [3].

Some small improvements are still possible, but the actual injection system is showing its limits to reduce these perturbations and also to obtain the ultimate goal to achieve a transparent injection with 100% efficiency. Many new injection systems have been proposed recently to solve this problem. One of these solutions is the use of an NLK which is the only one capable of providing fully transparent injection with multiple bunches as demonstrated in [4].

## PROPOSED INJECTION SCHEME

Figure 1 presents the present and the proposed injection schemes. The ESRF-EBS injection system is very similar to the one of the former machine. It is a standard off-axis injection scheme consisting of two in-air septa S1/2, one in-vacuum septum S3 and four kicker magnets K1 to K4 to generate the injection bump. To reduce the perturbations, the kickers have been equipped with a new power supply and the electro-magnet S2 septum has been replaced with a permanent magnet one.

The proposed injection scheme integrates an NLK magnet divided over 2 or 3 segments (2 segments in Figure 1) to provide the last deflection after S3 and bring the injected beam into the acceptance [5].

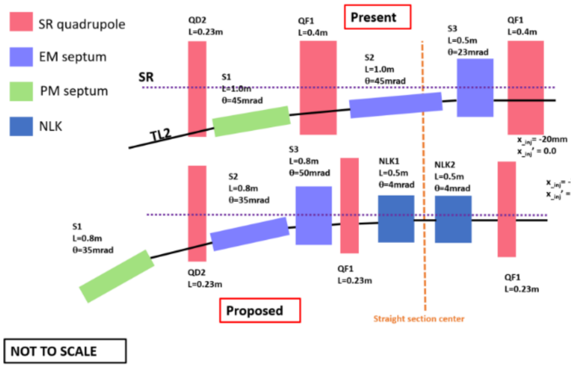

Figure 1: Proposed schemas for transfer line TL2 and storage ring injection straight to integrate NLKs.

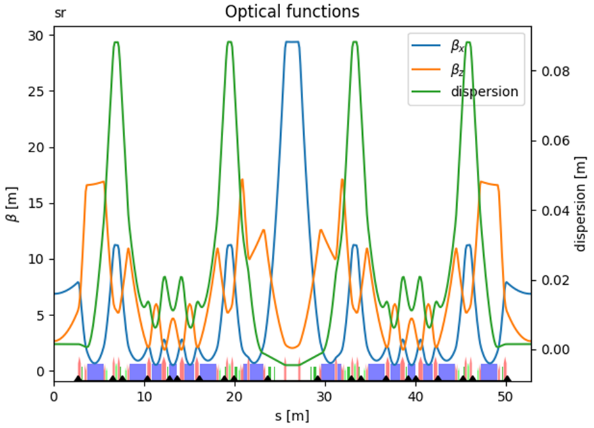

Figure 2: Lattice with NLK.

The total deviation angle of the NLK is 8 mrad. Due to this large angle, we need to inject on the peak field of the magnet. The distance between the two QF1 quadrupoles has been modified to allow the installation of all the NLK segments. The new lattice design (Fig. 2) is driven by the mechanical integration in order to optimize the space and also to achieve an easier kick for large distance between the stored and injected beams. The two QF1 quadrupoles are replaced with two EBS quadrupoles which are two times thinner (from 0.4 m to 0.23 m). The length of the septa has been modified, and permanent magnet technology will be used for septum S1.

## DESIGN OF THE NON-LINEAR KICKER

The idea of using a magnetic field distribution for the injection kicker with a magnetic field strength at a certain distance from the stored beam to bend the injected beam into the storage ring acceptance, and a zero-field strength in the centre to do not perturb the stored beam, was developed and implemented in different facilities. This concept has been introduced by KEK in a form of a pulsed quadrupole injection kicker [6], later further as a form of pulsed sextupole injection kicker [7]. Taking benefit from these developments, BESSY developed a pulsed octupole like injection kicker [8]. Other facilities have adopted similar concept for their injection kickers.

The ESRF-EBS NLK is based on the BESSY concept, its main parameters are given in table 1.

Table 1: Main Parameters of the ESRF-EBS NLK

| Description | Parameter |
|---|---|
| Number of conductors | 8 |
| Conductor Diameter | 2 mm |
| Deflection angle at 8 mm | 4 mrad |
| Peak Field at 8 mm | 0.17 T |
| Zero field region | ± 0.4 mm |
| Magnetic length | 0.5 m |
| Current | 5.5 kA |
| Current pulse length | 5.6 µs, half sine pulse |

The magnetic design of the NLK is based on eight copper wires with 2 mm diameter, each two wires are installed in a quadrant powered with opposite currents.

Figure 3 presents the horizontal and vertical position of the wires which allowed to obtained the required magnetic field at the injection position and also a zero field with a plateau at the stored beam position. Unlike BESSY's design, the position of the outer wires (3.7mm from the vertical axe) is smaller than the position of the inner wires (4.25 mm). This modification allows to have a magnetic field at the injection position with a less sharped shape, than less sextupole components, which is mandatory for our injected beam with relatively high emittance.

The magnetic simulations are done with COMSOL [9] software using the Frequency Domain Model. Figure 4 presents the distribution of the vertical magnetic field which is an octupole like shape. It is obtained with a vertical mirror symmetrical geometry of the four wires. The peak of the magnetic field (0.17 T) where the injected beam will be kicked is obtained at a distance of 8 mm from the position of the stored beam. The zero-field region where the stored beam will pass is a plateau with a very low magnetic field of $5.10^{-5}$ T within ± 0.4 mm in the transverse position.

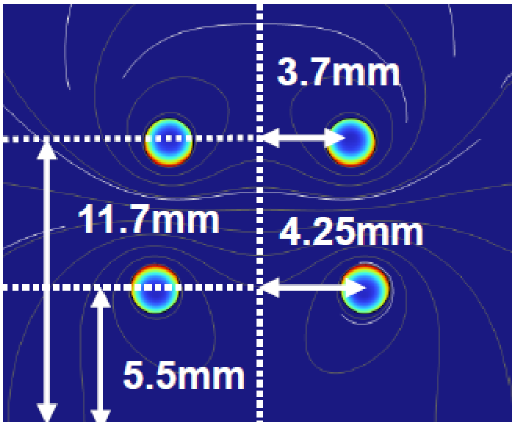

Figure 3: Current density distribution in the wires and theirs horizontal and vertical position from the storage beam axis.

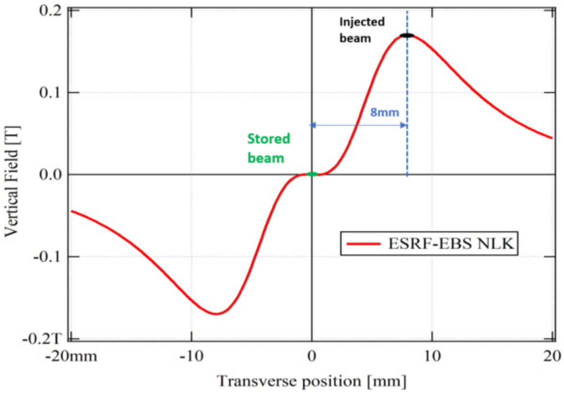

Figure 4: Octupole like magnetic field distribution with a peak field at 8 mm from the storage beam position.

The zero-field region where the stored beam passes without any perturbation is very sensitive to the mechanical position of the wires. A bad position of one or several wires breaks the mirror symmetrical geometry of the NLK and generates a magnetic field in the centre which perturbs the stored beam position. Table 2 presents the integrated dipole and quadrupole field components generated by introducing random errors on the wires position in the horizontal and vertical direction. We can remark that the residual magnetic field is proportional to the position error value, and even for a small position error of 20 µm which is the standard mechanical machining tolerance the residual angle is not negligible. The dipole errors can be compensated by the present active correction system. However, the quadrupole errors cannot be compensated.

Table 3 presents the integrated dipole and quadrupole field generated in the centre of magnet when a 20 µm translation systematic errors (in horizontal X and vertical Y directions) is applied on the four wires together, assuming that the other four wires are fixed.

Table 2: Dipole and Quadrupole Integrated Fields Generated by Random Conductor Wires Errors Position

| **Random errors** | **± 20µm** | **± 30µm** |
|---|---|---|
| $B_{y0}L$ [µrad] | 12 | 18 |
| $B_{x0}L$ [µrad] | -18 | -27 |
| GL [mT] | 5.1 | 7 |
| $G_sL$ [mT] | 2.9 | 4.3 |

Table 3: Dipole and Quadrupole Integrated Fields Generated by Systematic Conductor Wires Errors Position

| **Syst. errors** | **X** | **Y** |
|---|---|---|
| $B_{y0}L$ [µrad] | 0.08 | 0.1 |
| $B_{x0}L$ [µrad] | 0.17 | -0.1 |
| GL [mT] | 1 | 49 |
| $G_sL$ [mT] | -36.6 | -3.6 |

The integrated quadrupole GL and skew quadrupole $G_sL$ are very high and need to be compensated to avoid any perturbation on the stored beam.

## NON-LINEAR KICKER PROTOTYPE

Figure 5 presents the proposed NLK to perform copper wires assembly and magnetic measurement tests.

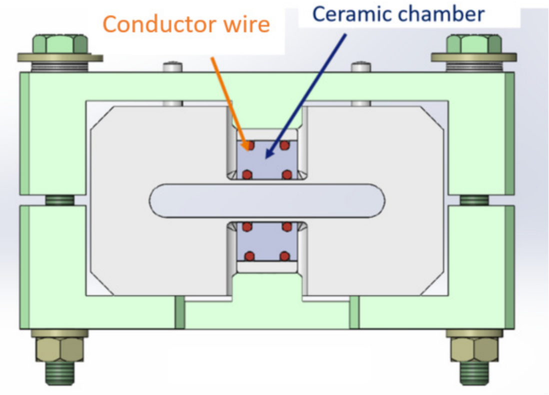

Figure 5: NLK prototype.

The production of the ceramic chamber is in progress. The conductor wires will be placed in a precisely machined grooves on this ceramic chamber. When powered, a magnetic force of 700 N is applied on each conductor wire. A mechanical system maintains the conductor wires in their places. Due the high sensitivity of NLK magnetic field in the centre, the position of the top part (four conductor wires together) can be adjusted by using non-magnetic and non-conductor shims in both translation or rotation displacement. The magnet is powered with a pulsed power supply producing a 5.5 kA in a shape of a half sine.

The NLK design, production and assembly needs to be validated with precise magnetic measurements. An adaptation of an existing stretched wire magnetic bench is in progress. It includes the equipment with stretched wires to measure varying fields, mechanical supports parts, control, data acquisition and analyse applications.

## CONCLUSION

A new injection scheme using NLK were proposed in order to reduce the injection perturbations and to obtain the ultimate goal which is achieving a transparent injection with 100% efficiency. An NLK design based on 8 conductors wires distributed and powered in a way to produce an octupole like magnetic field with a peak field at the injected beam and zero field at the stored beam. Residual magnetic field induced from position errors of the conductor wires were calculated. A prototype magnet will be assembled and characterised using the stretched wire magnetic bench.

## REFERENCES

[1] P. Raimondi, “Hybrid Multi Bend Achromat: from SuperB to EBS”, in *Proc. IPAC'17*, Copenhagen, Denmark, May 2017, pp. 3670-3675. `doi:10.18429/JACoW-IPAC2017-THPPA3`

[2] P. Raimondi *et al.*, “Commissioning of the hybrid multibend achromat lattice at the European Synchrotron Radiation Facility,” *Phys. Rev. Accel. Beams*, vol. 24, no. 11, Nov. 2021. `doi:10.1103/physrevaccelbeams.24.110701`

[3] S. M. White *et al.*, “Commissioning of New Kicker Power Supplies to Improve Injection Perturbations at the ESRF”, in *Proc. IPAC'22*, Bangkok, Thailand, Jun. 2022, pp. 2683-2685. `doi:10.18429/JACoW-IPAC2022-THPOPT041`

[4] P. Alexandre *et al.*, “Transparent top-up injection into a fourth-generation storage ring,” *Nucl. Instrum. Methods Phys. Res., Sect. A*, vol. 986, p. 164739, Jan. 2021. `doi:10.1016/j.nima.2020.164739`

[5] S. M. White and T. P. Perron, “Injection Using a Non-Linear Kicker at the ESRF”, in *Proc. IPAC'22*, Bangkok, Thailand, Jun. 2022, pp. 2679-2682. `doi:10.18429/JACoW-IPAC2022-THPOPT040`

[6] K. Harada, Y. Kobayashi, T. Miyajima, and S. Nagahashi, “New injection scheme using a pulsed quadrupole magnet in electron storage rings,” Physical Review Special Topics - Accelerators and Beams, vol. 10, no. 12, Dec. 2007. `doi:10.1103/physrevstab.10.123501`

[7] H. Takaki *et al.*, “Beam injection with a pulsed sextupole magnet in an electron storage ring,” Physical Review Special Topics - Accelerators and Beams, vol. 13, no. 2, Feb. 2010. `doi:10.1103/physrevstab.13.020705`

[8] T. Atkinson, M. Dirsat, O. Dressler, P. Kuske, and H. Rast, “Development of a Non-Linear Kicker System to Facilitate a New Injection Scheme for the BESSY II Storage Ring”, in *Proc. IPAC'11*, San Sebastian, Spain, Sep. 2011, paper THPO024, pp. 3394-3396.

[9] COMSOL Multiphysics Software, `https://www.comsol.com`